33rd Annual International Conference of the IEEE EMBS
Boston, Massachusetts USA, August 30 - September 3, 2011

Simulating Electrical Stimulation of Degenerative Retinal Ganglion Cells with Bi-phasic Pulse Trains

Tatiana Kameneva[1,*], David B. Grayden[1,2,3], Hamish Meffin[1,3] and Anthony N. Burkitt[1,2,3]

Abstract— **The aim of this work was to investigate how retinal ganglion cells (RGCs) respond to repetitive electrical stimulation in degenerative retina. The response of modeled ON and OFF cells was examined to bi-phasic pulse train stimulation of varying frequencies. Previously developed models of RGCs were extended to include an experimentally observable balance of excitatory and inhibitory currents in degenerative retina. The phenomena of fading and dark phosphenes with retinal implants were investigated. A hypothesis for a mechanism contributing to these phenomena was formulated.**

I. INTRODUCTION

Various features of visual information are encoded by different types of neurons in the retina. For example, ON retinal ganglion cells (RGCs) respond with a transient burst of spikes to light onset, while OFF RGCs respond with a sustained burst of impulses at the light offset [6].

In visually impaired people who have lost their photoreceptors due to inherited diseases, a large number of RGCs survive [10]. A sensation of light for these people can be elicited by excitation of RGCs with electrical stimulation (these are usually roundish spots of light called phosphenes) [7]. For a successful employment of a visual prosthesis, it may be important to mimic natural information transfer in the retina and differentially stimulate different types of RGCs with electrical stimulation. Some forms of selective stimulation of neurons in the retina have been shown *in-vitro* [3], [11]; however, little is known about how the differential stimulation of RGCs affects patients with retinal implants.

Another important area of research involving retinal implants is the investigation of the phenomena of fading and dark phosphenes that has been reported by some patients [2], [16]. When patients are presented with a high frequency pulse train, perception of the second (and succeeding) pulses is diminished (faded). At sufficiently high frequencies, patients report seeing only an initial phosphene. Fading increases sharply when inter-pulse intervals are shorter than 155 ms [16]. Additional factors may affect fading, including placement of the implant (epiretinally vs. subretinally). As well as fading, some subjects report seeing dark phosphenes (perceived spots darker than background) with high frequency pulse stimulation (20 pulses per second) [2].

Consistent with psychophysical data, *in-vitro* data indicates that the response of ganglion cells decreases for subsequent pulses when stimulating at a high frequency. It has been shown that when the inter-pulse interval is 100 ms, the response to the second pulse is reduced by 40% [5]. When the inter-pulse interval is 25 ms, the response to the second pulse is abolished [5]. This study did not differentiate between ON and OFF RGCs. In contrast to [5], other studies demostrated a response of RGCs to high frequency pulses [4], [13].

In this paper, we investigate a possibility that differential stimulation of ON and OFF RGCs accounts for the phenomena of fading and dark phosphenes. We hypothesize that the phenomena of fading and dark phosphenes are due to higher spiking rate of OFF cells than ON cells, which compromises the information decoding ability of neurons in visual cortex. The response of modeled ON and OFF ganglion cells is analyzed for pulse trains of varying frequency using well-constrained models of each cell type. The proposed hypothesis is supported by examining the spiking rate of modeled ON and OFF cells with stimulation by pulse trains of varying frequency.

II. METHODS

A. Model constraints

Numerical simulations of single-compartment Hodgkin-Huxley-type neurons were carried out in NEURON. The equation governing changes in the membrane potential, V, with time, t, was obtained by summing all membrane and synaptic currents using Kirchoff's law:

$$C_{\mathrm{m}}\frac{dV}{dt} + I_{\mathrm{Na}} + I_{\mathrm{Ca}} + I_{\mathrm{K,A}} + I_{\mathrm{K(Ca)}} + I_{\mathrm{K}} + I_{\mathrm{T}} + I_{\mathrm{h}} + I_{\mathrm{NaP}} + I_{\mathrm{L}} + I_{\mathrm{Inh}} + I_{\mathrm{Exc}} + I_{\mathrm{Stim}} = 0. \quad (1)$$

The dynamics of each voltage-gated ion current are governed by Hodgkin-Huxley-type gating variables, which are described by first-order kinetic equations as given in [1] (for $I_{\mathrm{Na}}, I_{\mathrm{Ca}}, I_{\mathrm{K,A}}, I_{\mathrm{K(Ca)}}$ and I_{K}), [14] (for I_{T}), [15] (for I_{h}) and [12] (for I_{NaP}), but are omitted here for brevity. The dynamics of synaptic currents I_{Inh} and I_{Exc} are described in the next section. C_{m} is the specific capacitance of the membrane. I_{Stim} is an intracellular stimulation current. The models of ON and OFF cells were constrained based on the intrinsic electrophysiology of ON and OFF RGCs when all synaptic inputs are blocked. The models were based on experimental data in mice; it was shown that intrinsic properties of RGCs are maintained in RD mice, even into late-stage retinal degeneration [9].

Using the constraints, two distinct sets of the parameters $(\bar{g}_{\mathrm{h}}, \bar{g}_{\mathrm{T}}, \bar{g}_{\mathrm{NaP}})$ were found that correspond to ON and OFF cells populations. Broadly speaking, the ON set constraints are satisfied for conductances in the following ranges: $\bar{g}_{\mathrm{h}} \leq$

[1] Department of Electrical and Electronic Engineering, The University of Melbourne. [2] The Bionics Institute. [3] NICTA Victoria Research Labs. *Corresponding author, tkam@unimelb.edu.au.

10^{-6} S/cm^2, $\bar{g}_{\rm NaP} \le 10^{-6}$ S/cm^2, $\bar{g}_{\rm T} = 0$ S/cm^2. The OFF set constraints are satisfied for conductances in the ranges: $\bar{g}_{\rm h} \le 10^{-6}$ S/cm^2, $\bar{g}_{\rm NaP} \le 10^{-6}$ S/cm^2 and $\bar{g}_{\rm T} \in [10^{-3} - r_-, 10^{-3} + r_+]$ S/cm^2, where r_- and r_+ are relatively small compared to 10^{-3} and depend on $\bar{g}_{\rm h}$ and $\bar{g}_{\rm NaP}$. For details of how the model was constrained, refer to [8].

We extend the model [8] by including the excitatory and inhibitory currents. In the absence of sensory input, the resting spike activity of RGCs in normal retina is irregular. However, in retinal degeneration (RD), rhythmic synaptic input drives ongoing oscillatory firing in ON and OFF RGCs at a frequency of approximately 10 Hz [9]. Maintained rhythmic activity is not synchronized between RGCs and is a characteristic feature of RD RGCs that is not seen in normal retinae. In addition, the balance of inhibitory and excitatory input is different for ON and OFF RGCs: ON cells receive 10-fold weaker inhibition than OFF cells. The models of OFF and ON cells with added synaptic currents were constrained to reproduce maintained rhythmic spiking rate based on data in [9]: rhythmic bursts of spikes every 100 ms for ON and OFF cells, spiking rate for ON RGCs 22 ± 5 Hz and for OFF RGCs 29 ± 11 Hz. The dynamics of the inhibitory and excitatory currents are described by:

$$I_{\rm Inh} = g_{\rm Inh}(t)(V - V_{\rm Inh}) \quad (2)$$

$$I_{\rm Exc} = g_{\rm Inh}(t)(V - V_{\rm Exc}), \quad (3)$$

where $V_{\rm Inh} = -70$ mV and $V_{\rm Exc} = 0$ mV are the reversal potentials for the inhibitory and excitatory currents, respectively. $g_{\rm Inh}, g_{\rm Exc}$ are the time-varying conductances that were fit to the experimental data [9] (refer to Fig. 2b) using the polynomial curves:

$$g_{\rm Inh}(t) = a_1 e^{-\left(\frac{t-b_1}{c_1}\right)^2} + a_2 e^{-\left(\frac{t-b_2}{c_2}\right)^2} + a_3 e^{-\left(\frac{t-b_3}{c_3}\right)^2} \quad (4)$$

$$g_{\rm Exc}(t) = (p_1 t^2 + p_2 t + p_3)/(t^2 + q_1 t + q_2). \quad (5)$$

The values for $g_{\rm Inh}$, $g_{\rm Exc}$ were repeated for $t = t + k \cdot 100$ms, $k = 1, 2, \ldots$ to replicate periodic functions. The values of coefficients were as follows. For OFF cells: $a_1 = 0.52, a_2 = 0.54, a_3 = 0.2, b_1 = 49.95, b_2 = 50.05, b_3 = 49.78, c_1 = 2.99, c_2 = 18.71, c_3 = 31.36$. For ON cells: $p_1 = 0.03, p_2 = -3.03, p_3 = -16.85, q_1 = -100, q_2 = 2775$. For OFF cells: $p_1 = 0.04, p_2 = -3.72, p_3 = -20.76, q_1 = -99.18, q_2 = 2978$. The coefficients were statistically significant at the 95% confidence level. Based on experimental evidence [9], our model does not include inhibitory current for ON cells.

Polynomial fits (4) and (5) were based on data in [9, Fig. 5]. Due to difficulties in determining the amplitude scale of synaptic currents in the experimental data (Fig. 5 vs Supplementary Fig. 3 in [9]), the amplitude of each synaptic current was multiplied by 0.4 to reproduce the experimentally measured spiking rate of ON and OFF cells. The phase shift between inhibitory and excitatory currents in OFF RGCs was chosen to match experimental data presented in [9, Fig. 5]. In simulation, the standard Euler numerical integration method with time step 0.025 ms was used. All voltage-dependent parameters were initialized at a membrane potential of -65 mV.

B. Pulse stimulation

The constrained model with synaptic currents was used to investigate responses of ON and OFF RGCs to the voltage stimulation used in [16]. The voltage pulse stimulation was approximated by a charge-balanced current stimulation. An approximated current stimulation is shown in dashed red in Fig. 1; however, for simplicity, we use rectangular pulses shown in solid black in Fig 1. This simplification does not affect qualitative results. It was assumed that stimulation current that passes across the membrane, $I_{\rm Stim}$ in (1), is proportional to the current being passed through the extracellular stimulation electrodes. Duration of the anodic phase,

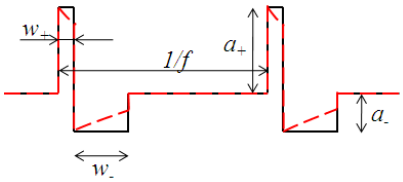

Fig. 1. Pulse train stimulation. Dashed (red online): bi-phasic current clamp stimulation as an approximation to voltage pulse stimulation used in [16]. Solid: simplified approximation by a rectangular bi-phasic current clamp that was used in simulation. Parameters used in simulations: $w_+ = 3$ ms, $w_- = 10$ ms, $a_- = a_+ w_+ / w_-$ nA, $a_+ \in [0.4, 1.6]$ nA, $1/f \in [15, 425]$ ms.

w_+, was set to 3 ms similar to [16]. Duration of the cathodic phase, w_-, was set to 10 ms to represent the charge recovery time. To explore the responses of the model neurons to trains of pulses of different frequencies and amplitudes, the amplitude of the cathodic phase, a_+, was varied from 0.4 nA to 3 nA with a linear step size of 0.02 nA. The interpulse interval, $1/f$ (f corresponds to the frequency of the pulse train), was varied from 15 ms to 425 ms (similar to [16]) with a linear step size of 10 ms. The amplitude of the anodic phase, $a_- = a_+ w_+ / w_-$, was adjusted to keep charge balance. The interphase gap was set to zero. The duration of a pulse train was 2 sec.

The parameter space of interpulse frequency and the cathodic amplitude of the bi-phasic current pulses was systematically explored with stimulations of ON and OFF RGCs. The spiking rate was averaged over six different ON and six different OFF cells respectively. The values of maximum conductances for $I_{\rm Na}, I_{\rm Ca}, I_{\rm K,A}, I_{\rm K(Ca)}$, $I_{\rm K}$, and $I_{\rm L}$ for these cells were set the same as in [1]. For OFF cells, $g_{\rm NaP}, g_{\rm T}, g_{\rm h}$ were set the same as for the cells used for averaging in [8]. For ON cells, $g_{\rm NaP} = 5 \cdot 10^{-8}$ S/cm^2, $g_{\rm T} = 0$ S/cm^2, $g_{\rm h} \in [2 \cdot 10^{-7}, 1.5 \cdot 10^{-6}]$ S/cm^2 with step size factor of 1.5. To measure the relative spiking rate of ON and OFF RGCs, the difference between spiking rate, Δ, was calculated according to the formula:

$$\Delta = (R_{\rm OFF} - R_{\rm OFFSpont}) - (R_{\rm ON} - R_{\rm ONSpont}), \quad (6)$$

were $R_{\rm OFF}, R_{\rm ON}$ are the respective spiking rates of OFF and ON RGCs with a repetitive pulse stimulation, and $R_{\rm OFFSpont}, R_{\rm ONSpont}$ are the respective maintained spiking rates of OFF and ON RGCs.

III. RESULTS

A. Model constraints

Modelled synaptic currents for ON and OFF RGCs are shown in Fig. 2a. Experimentally measured inhibitory and excitatory currents are shown in Fig. 2b for comparison [9]. Three traces in Fig. 2a show the modeled excitatory current for ON cell and the inhibitory and excitatory currents for OFF cells. Based on [9], the amplitude of the inhibitory current in ON cells is significantly smaller than the amplitude of the excitatory synaptic current in ON cells and of inhibitory and excitatory currents in OFF cells. The inhibitory synaptic current in ON cells was neglected since it is much smaller than the other three synaptic currents. In Fig. 2b the top traces for ON and OFF cells are experimentally measured inhibitory currents, the bottom traces are excitatory currents, adapted from [9].

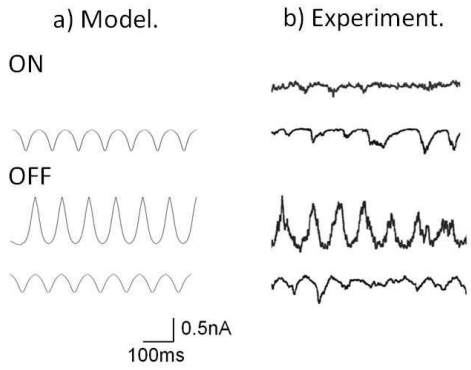

Fig. 2. A balance of synaptic currents in ON and OFF RGCs. A top trace for ON and OFF cells is an inhibitory current, a bottom trace is an excitatory current. a) Model results: polynomial curve fitting of data [9] in MATLAB^{TM} computing environment. b) Experimental results: modified from [9, Fig. 5a].

We were able to reproduce continuous rhythmic bursts of spikes in ON and OFF RGCs with an interburst beating frequency of 10 Hz. Simulations show that the average maintained firing rate for ON cells is 27 Hz and for OFF cells is 35 Hz, which corresponds well to the experimental data of the overall mean maintained rate of 22 ± 5 Hz for ON RGCs and 29 ± 11 Hz for OFF RGCs [9]. An example of modelled ON and OFF RGCs maintained activity is shown in Fig. 3a. The dynamics of the membrane potential of ON and OFF cells from patch-clamp experiments [9] is given in Fig. 3b for comparison.

B. Pulse stimulation

Simulation results giving the difference between OFF and ON RGCs' spiking rates as a function of the pulse frequency and cathodic phase amplitude are given in Fig. 4. Note, while the parameter space explored was $a_+ \in [0.4, 1.6]$ nA, Fig. 4 shows only the results for $a_+ \in [0.4, 0.8]$ nA. This range includes amplitudes of a cathodic phase, a_+, that gave hyperpolarization levels of the membrane potential in the range $[-83, -125]$ mV. Using amplitudes larger than

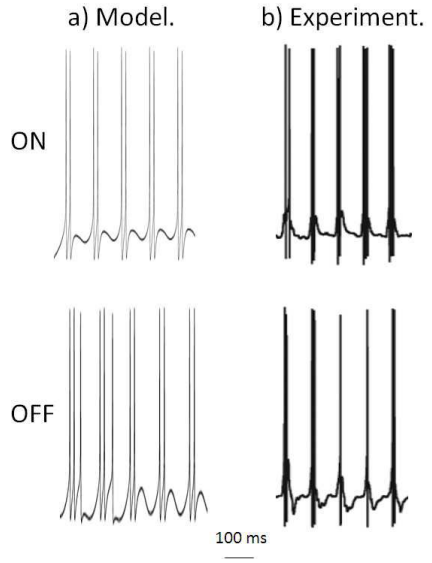

Fig. 3. Rhythmic resting spike activity of ON and OFF RGCs. a) Model results. b) Experimental results: modified from [9, Fig. 2b] for comparison.

0.8 nA hyperpolarized the cell to much lower levels. The contours in Fig. 4 show -100 mV and -120 mV levels of membrane hyperpolarization. The model predicts that with

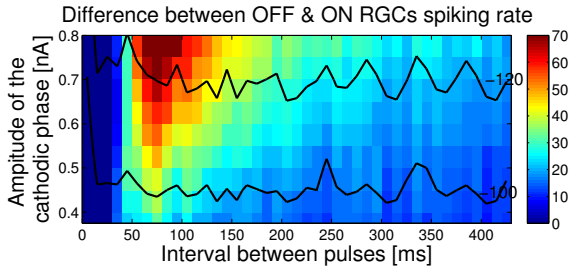

Fig. 4. Simulated spiking response of RGCs to a pulse train as a function of a pulse frequency (x-axis) and a cathodic phase amplitude (y-axis) of the injected current. The plotted spiking rate is the relative difference between OFF and ON RGCs calculated according to (6). The spiking rate in coded by the grey-scale (color online) shown on the right hand side of the plot. The contours on show -100 mV and -120 mV levels of membrane hyperpolarization.

pulse stimulation, OFF cells fire preferentially over ON cells when the pulse train frequency is between 10 and 20 Hz. The response of ON and OFF RGCs to 10 Hz frequency pulse stimulation is given in Fig. 5. The ON cell's spike rate is 34 Hz, compared with the OFF cell's spike rate of 60 Hz. The applied pulse train is superimposed and shown below the trace of the membrane potential. The prediction is based on OFF cells' bandpass response at around 10 Hz (data not shown). To check if the bandpass response was due to difference in synaptic balance or due to difference in maximum conductance of I_T between ON and OFF cells, we ran two additional sets of simulations: with swapped inhibitory and excitatory currents between ON and OFF cells (OFF cells had ON cells' synaptic currents and vice versa) and simulations with no synaptic currents included.

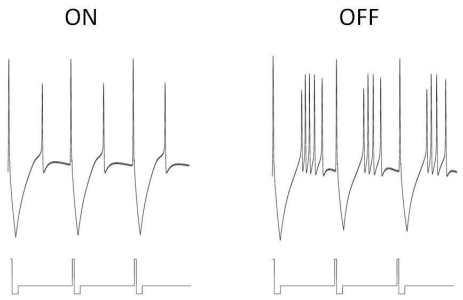

Fig. 5. ON and OFF RGCs simulated response to the bi-phasic pulse stimulation with the following parameters: $a_+ = 0.6$ nA, $w_+ = 3$ ms, $a_- = -0.18$ nA, $w_+ = 10$ ms, $f = 10$ Hz ($1/f = 100$ ms). The applied pulse train is superimposed and shown below the trace of the membrane potential. Time scale: interval between positive pulses is 100 ms.

In both cases, the bandpass response was present in OFF cells. Therefore, we conclude that this response is due to the difference in I_{T} between ON and OFF cells. At 10 Hz pulse frequency, with 10 ms duration of a cathodic phase, 30% of I_{T} currents are open (data not shown). Due to the absence of I_{T} in ON RGCs, this percentage is sufficient to generate the aforementioned phenomena.

Results show that it is possible to preferentially stimulate OFF RGCs using pulse trains of 10-20 Hz frequency. These results also support the proposed hypothesis of fading and dark phosthenes – that these phenomena are due to the dominance of OFF RGCs caused by a much higher spiking rate of OFF cells than of ON cells.

IV. DISCUSSION

Using a well-constrained model of ON and OFF RGCs with added synaptic currents, this work examined the response of RGCs to pulse stimulation. The ability of RGCs to follow repetitive pulse stimulation was investigated. Computer simulations predict that OFF cells spike preferentially over ON cells when a 10-20 Hz pulse train is applied. These findings may have substantial functional ramifications for the development of a retinal prosthesis. Finding a stimulus that mimics the healthy retina and can differentially target ON or OFF RGCs, depending on visual scene transmitted, may have many benefits for visual implant recipients. The model prediction remains to be checked experimentally.

Preferential stimulation of OFF cells may explain reports by patients of black phosphenes [2]. While our results also support the proposed hypothesis that higher spiking rate in OFF cells contribute to fading, it remains to explain underlying network and electrophysiological properties of the phenomena of fading. An adaptation of cells to the application of the repetitive pulses is an important issue to address in the future.

The 10 Hz preferential stimulation of OFF cells coincides with the frequency of synaptic input rhythmicity. This rhythmicity is not observed in healthy retina and may represent an intrinsic mechanism necessary for neuron survival in degenerative retina. It remains to be checked what phase shift between a pulse train and a synaptic input phase will produce maximum difference in ON and OFF cells' spiking rate.

Note, [4], [11], [13] were able to stimulate RGCs at much higher frequency (200 Hz and higher). It is left for future research to check if predictions of this study are altered when a network of retinal neurons is employed. It is also important to investigate the role of the cells' morphologies and intrinsic physiological properties of different types of ON and different types of OFF RGCs in responses to electrical stimulation.

V. ACKNOWLEDGMENTS

This research was supported by the Australian Research Council through its Special Research Initiative in Bionic Vision Science and Technology grant to Bionic Vision Australia. The Bionic Ear Institute acknowledges the support it receives from the Victorian Government through its Operational Infrastructure Support Program.

REFERENCES

[1] J. F. Fohlmeister and R. F. Miller. Impulse encoding menchanisms of ganglion cells in the tiger salamander retina. *J. Neurophysiol.,* 78: 1935 - 1947, 1997.

[2] A. Perez Fornoz, J. Sommerhalder, M. Pelizzone. Dynamics of visual perception upon electrical stimulation of the retina. *Assoc. for Research in Vis. and Ophtalm. Annual Conf.,* 2010.

[3] D.K. Freeman, D.K. Eddington, J.F. Rizzo, S.I. Fried. Selective activation of neuronal targets with sinusoidal electric stimulation. *J. Neurophysiol.,* 104: 2778 - 2791, 2010.

[4] S.I. Fried, H.A. Hsueh, F.S. Werblin. A method for generating precise temporal patterns of retinal spiking using prosthetic stimulation. *J. Neurophysiol.,* 95: 970 - 978, 2006.

[5] R.J. Jensen, J.F. Rizzo. Responses of ganglion cells to repetitive electrical stimulation of the retina. *J. Neural Eng.,* 4: S1 - S6, 2007.

[6] H.K. Hartline. Visual receptors and retinal interaction. *Science,* 164: 270 - 278, 1969.

[7] M.S. Humayun, E. de Juan, G. Dangnelie, R.J. Greenberg, R.H. Prospst, D.H. Phillips. Visual perception elicited by electrical stimulation of retina in blind humans. *Arch. Ophthalmol.,* 114: 40 - 46, 1996.

[8] T. Kameneva, H. Meffin, A.N. Burkitt. Modelling intrinsic electrophysiological properties of ON and OFF retinal ganglion cells. *In press: J. Comp. Neurosci.,* 2011. doi: 10.1007/s10827-011-0322-3.

[9] D.J. Margolis, G. Newkirk, T. Euler, P.B. Detwiler. Functional stability of retinal ganglion cells after degeneration-induced changes in synaptic input. *J. Neurosci.,* 28: 6526 - 6536, 2008.

[10] N.F. Medeiros, C.A. Curcio. Preservation of ganglion cell layer neurons in age-related macular degeneration. *Invest. Ophthalmol. Vis. Sci.,* 42: 795 - 803, 2001.

[11] C. Sekirnjak, P. Hottowy, A. Sher, W. Dabrowski, A.M. Litke, E.J. Chichilnisky. Electrical stimulation of mammalian retinal ganglion cells with multielectrode arrays. *J. Neurophysiol.,* 95: 3311 - 3327, 2006.

[12] R.D. Traub, E.H. Buhl, T. Gloveli, M.A. Whittington. Fast Rhythmic Bursting Can Be Induced in Layer 2/3 Cortical Neurons by Enhancing Persistent NaP Conductance or by Blocking BK Channels. *J. Neurophysiol.*, 89: 909 - 921, 2003.

[13] D. Tsai, J.W. Morley, G.J. Suaning, N.H. Lovell. Direct activation and temporal response properties of rabbit retinal ganglion cells following subretinal stimulation. *J. Neurophysiol.,* 102: 2982 - 2993, 2009.

[14] X.-J. Wang, J. Rinzel, M. Rogawski. A model of the T-type calcium current and the low-threshold spike in thalamic neurons. *J. Neurophysiol.,* 66: 839 - 850, 1991.

[15] I. van Welie, M. W. H. Remme, J. van Hooft, W. J. Wadman. Different levels of Ih determine distinct temporal integration in bursting and regular-spiking neurons in rat subiculum. *J. Physiol.,* 576.1: 203 - 214, 2006.

[16] R. G. Wilke, K. Stingl, E. Zrenner. Fading Of Perception In Retinal Implants Is A Function Of Time And Space Between Sites Of Stimulation. *Assoc. for Research in Vis. and Ophtalm. Annual Conf.,* 2011.